

TECHNICAL ARTICLE

Investigation on the Efficient Removal of Particulate Matter (PM) with Biomass-Based Aerogel

Yixin Wang*, Emmanuel Tapia-Brito*, James Riffat*, Ziwei Chen*, Fatang Jiang*[†] and Saffa Riffat*

Biomass-based aerogel is a new promising environmentally friendly filter material to remove fine particle matter and minimize air pollution. This study aims to investigate the air filtration properties of biomass-based aerogels via tests in a transparent chamber and verification in a real room with a burning smudge stick as a the particle source. The biomass-based aerogel used in this study is made of polysaccharides, protein and waste agricultural by-product (wheat straw). The addition of wheat straw contributes to the increase of surface area and complexity of the biomass-based aerogel pore structure. Compared with other commonly used commercial filtration materials including high-efficiency particulate air (HEPA) filter, surgical mask, regular cloth and silica aerogel, biomass-based aerogel K0.9G1.8S3.6WS1.8 shows excellent performance to remove PM 2.5 (99.50%) and PM 10 (99.40%) from the environment. When using the biomass-based aerogel, the filter core sample has a smaller volume and simpler structure than HEPA to achieve the similar filtration performance. The filtration performance of the biomass-based aerogels has been verified with a real room test. The current work demonstrates the high potential of biomass-based aerogels for infiltration application in different fields and provides an avenue to reuse agricultural by-products.

Keywords: Biomass-based aerogel; Air filtration; PM capture; Air quality

1. Introduction

Recently, air pollution is one of the main environmental problems in the world and is among the critical challenges facing modern societies. It refers to the contamination of the atmosphere by a mix of hazardous substances, particulate matter (PM) from natural sources and human activities. Natural forms of pollution are those that result from naturally occurring phenomena, such as volcanic eruptions, forest fire, ocean waves, soil dust. But the greatest contributor to pollution is human activities including industrial waste exhaust gas, fossil-fuel emissions, motor vehicle emissions, etc. Inhalable PM particles can be roughly divided into two size fractions PM 2.5 (aerodynamic diameter below 2.5 μm) and PM 10 (aerodynamic diameter between 2.5 μm and 10 μm) (Meng, Zhang, Yang, Yang, & Zhou 2016; Zoran, Savastru, Savastru, & Tautan 2020), both of those are fine inhalable particles and cannot be detected by naked eyes so that they are easily

inhaled into human lung contributing to serious health problems (Zhang et al. 2018). Between them, particles with a diameter less than 2.5 μm , which is only 3% of the diameter of a human hair, are also known as PM 2.5. They are easier to penetrate deep into the human lungs and some may even enter the bloodstream and circulatory system, causing cough and asthma, or even morbidity and mortality.

To solve this serious problem, researchers from all over the world are dedicated to studying various techniques to reduce air pollution. In the early period, the filter materials were mainly made of cotton, wool, jute, various synthetic fabrics of cellulose and other porous fabrics. Mandal and Srimani (1987) have used jute fiber as the filter in the microbiological experiment. In the 1940s, the high-efficiency particulate air (HEPA) filter was invented in the USA (Zare Shahneh 2020) and then it was introduced into commercial applications in the following decade, such as air purification in special rooms. Since then, filter materials have developed rapidly and grown in popularity and necessity. In recent years, there are many novel air filter materials appeared in succession. Filtration materials are widely used in many applications including the typical heating ventilation and air conditioning (HVAC) systems, HEPA is also popular in the manufacture of face masks and personal protective equipment (PPE) during the

* Faculty of Engineering, University of Nottingham, UK

[†] Glyn O. Phillips Hydrocolloid Research Centre at HBUT, National "111" Center for Cellular Regulation and Molecular Pharmaceutics, School of Food and Biological Engineering, Hubei University of Technology, CN

Corresponding author: Emmanuel Tapia-Brito (b_tapia@hotmail.com)

COVID-19 pandemic. Hui Liu et al. (2020) created a kind of nanoscale polyacrylonitrile fiber filter using an innovative electrospinning technique. It has been verified that the PM 0.3 was reduced by 99.99% with the novel nanonet filter. Abdul Rajak et al. (2020) used expanded polystyrene (EPS) waste as the raw material to make a nanofibrous membranes filter through the electrospinning method. Such nanofibrous membranes with low density and high Young's modulus can achieve high-efficiency PM 2.5 removal of 99.99% and a high-quality factor of 0.15 Pa^{-1} . Chao Jia et al. (2020) developed a kind of Al_2O_3 -stabilized ZrO_2 submicron fiber air filter paper, which has high filtration efficiency (99.56%) and a low-pressure drop (108 Pa). At the same time, this material also shows excellent flexibility and thermal stability. Using the electrostatic induction-assisted solution blowing method, Shengnan Lv et al. (2018) fabricated PLA/PMMA composite nanofibers with 99.5% PM 2.5 removal. In the research of Wallace Woon FongLeung and Qiangqiang Sun, the improved nanofiber filter with charged fibers has been invented for capturing 100 nm aerosols, which are similar to that of the COVID-19 (Leung & Sun 2020).

Moreover, to date, most of the current filtration materials are 2D materials rather than 3D materials and the disposal process after usage has been rarely considered as some of them are harmful to the environment (Zhang et al. 2018). Recently, various 3D-structured aerogels are widely used as adsorption materials due to their porous structure, 3D network structure and large surface area (Wang et al. 2019; Wang, Chen, et al. 2019; Wang et al. 2018). The types of existing aerogel filtration materials are complex, such as graphene aerogel filter (Zhao et al. 2020), MoS_2 carbonized cellulose aerogel (Xie et al. 2021), polyimide nanofiber assembled aerogel (Qiao et al. 2021), etc. Furthermore, due to the limitation in the preparation of the aerogel filters, many of them are toxic and difficult to degrade in nature. To solve this, it has been applied the use of some nature-derived materials as the raw materials to produce aerogels, including cellulose (Li & Fu 2021), chitosan (Yin, Sun, Bao, & Li 2020), pectin (Groult, Buwalda, & Budtova 2021), alginate (Zhuang et al. 2020), starch (Ubeyitogullari & Ciftci 2016), gum arabic (L. Wang, Sánchez-Soto, & Abt 2016) whey protein (Buggy, McManus, Brodkorb, Hogan, & Fenelon 2018), egg white protein (Selmer, Kleemann, Kulozik, Heinrich, & Smirnova 2015), etc. Based on previous research, there are two main preparation methods used to manufacture biomass-based aerogels, the supercritical drying method and the freeze-drying method. Nowadays, it is a tendency that more and more studies are preferring to use the freeze-drying method because of its low cost and high safety. Freeze drying is a low-temperature dehydration process that the gelled sol is frozen and then dried through the sublimation process under a high vacuum. Konjac glucomannan (KGM) is a neutral heteropolysaccharide, its main chain composed of d- glucose (G) and d- mannoses (M) in a molar ratio of 1:1.6 linked by β -(1,4)-glycosidic bond (Behera & Ray 2016). Starch (Wang, Su, et al. 2019) is a polymeric carbohydrate consisting of glucose, which can be classified into two kinds depending on the structure, i.e., amylose and amylopectin. Known

as a kind of high molecular weight polypeptide, gelatin is widely used in many fields. Gelatin is derived from the partial hydrolysis of collagen, which is extracted from the animal byproduct (Guilherme et al. 2021) and it has a distinctive structure (Ge, Wu, Woshnak, & Mitmesser 2021). Wheat straw is an agricultural waste with low-cost renewable feedstocks that has the potential to be used in aerogel manufacture. Based on current serious situation of the COVID-19 pandemic, more attention has been placed on the air quality issues. Therefore, an attempt was made to find what is the best way to improve air quality by removing particles and apply filtration materials in different fields, such as HVAC systems in buildings, face masks, etc. Some current filter materials are not bio-degradable and may harm the environment. However, with the use of biomass materials, such as biomass-based aerogels, particles can be filtered and removed in an environmentally friendly way. By testing the particle number before and after the flow passing through the materials in an airtight negative pressure environment, Wu et al. (2021) studied the filtration performance of biomass-based aerogels of single layer and combined multilayers and the results show that the higher solid concentration of single layer biomass-based aerogel and the combination of aerogel pieces with different pore size distribution contribute to better filtration efficiency. Although the above research revealed the filtration performance of biomass-based aerogel in standard tests, the testing method and results have a limitation that the long-time filtration performance is not able to be reflected. This long-time performance is significantly meaningful when the filtration materials are used in practical applications. This study aims to test the air filtration properties of new biomass-based aerogels in a long period, an environmentally friendly and efficient filter, compared with other common commercial filtration materials including HEPA, surgical mask, regular cloth and silica aerogel. A purifier fitted with different types of filters, a testing chamber and a real room have been developed to simulate the air polluted environment and to test the PM removal ability of different materials.

2. Materials and methods

2.1. Materials

KGM was provided by Licheng Biological Technology Co., Ltd. (Wuhan, China). Potato starch powder was obtained by Wuhan Lin He Ji Food Co., Ltd (Wuhan, China). Gelatin was purchased from Sinopharm Chemical Reagent Co., Ltd. (Shanghai, China).

2.2. Sol-gel solution preparation

The biomass-based aerogel was produced from KGM, gelatin, starch and wheat straw using the freeze drying method (Wu et al., 2021). This preparation method is based on three patents (Jiang 2013; Jiang 2020a; Jiang 2020b) and the previous research (Wang et al. 2018). The gelatin particles were dissolved in water with water bathing at 60°C for 0.5 h. After dissolved totally, the water bath temperature was increased to 95°C , and then potato starch, wheat straw and KGM were gradually added and mixed with stirring speed of 600 rpm for one hour. In this research,

there are three different solid concentrations selected and presented in **Table 1**. K, S, G and WS represent konjac glucomannan, potato starch, gelatin, wheat straw, respectively; the number after K, S, G and WS indicates the weight volume percent of composition in the original sol. Subsequently, the sol was injected into a cylindrical cell culture (15 cm) precooling and aging at 4°C.

2.3. Biomass-based aerogel preparation

After the aging process, the gel was frozen using an ultra-low temperature freezer (LGT 2325, Liebherr Ltd) at -25°C for 10 h. Once completely frozen, the samples were placed in a freeze dryer (FD-1A-50, Biocool Ltd) drying at -55°C under a vacuum of one Pa for approximately 24 h to obtain biomass-based aerogel samples.

2.4. Characterization of different filters

2.4.1. Microstructure observation with digital microscope

For the internal structure observation, the lab-scale KERN OBL 135C825 digital compound microscope with the adapted camera (ODC 825) has been used to observe the

materials and take photos. All samples were cut into a small strip with the size of 4 cm * 2 cm. The eyepiece lens magnification is 10x/Ø20 mm. The observation of different materials is carried out at the objective magnifications of 4x and 10x.

2.4.2. Microstructure observation with Scanning Electron Microscope

Scanning Electron Microscopes (SEM) can be used to visualise the internal structure of different filters before and after PM capture. The tests were carried out at magnifications of x50, x200 and x500 with an SEM (JEOL LV6060, Tokyo, Japan). The filter samples were coated with gold particles using a Gold and Platinum Sputter Coater.

2.4.3. PM generation and filtration measurements

To quantify the efficiency of PM filtration, a burning smudge stick was used as the source of PM particles. With a continuous supply, different sizes of particles will be produced for the test. The filtration efficiency of PM is measured using the apparatus shown in **Figure 1**. All the tests were implemented in a transparent chamber. On one side, an access door was set for changing samples. To provide a steady smog source, a small fan was placed on the left of the chamber and next to the burning smudge stick. Samples were cut as a disc with a diameter of 73 mm and used as the core of air purifier (B-D01, Acekool Portable Air Purifier). All samples were inserted into the plastic ring groove as shown in **Figure 2**. After passing through purifier, most of the PM 2.5 and PM 10 particles were intercepted by the filter materials, and the remain-

Table 1: The formula of the samples and their raw materials.

Sample Code	(g/100 mL)			
	KGM	Gelatin	Starch	Wheat straw
K0.5G1S2WS1	0.5	1	2	1
K0.7G1.4S2.8WS1.4	0.7	1.4	2.8	1.4
K0.9G1.8S3.6WS1.8	0.9	1.8	3.6	1.8

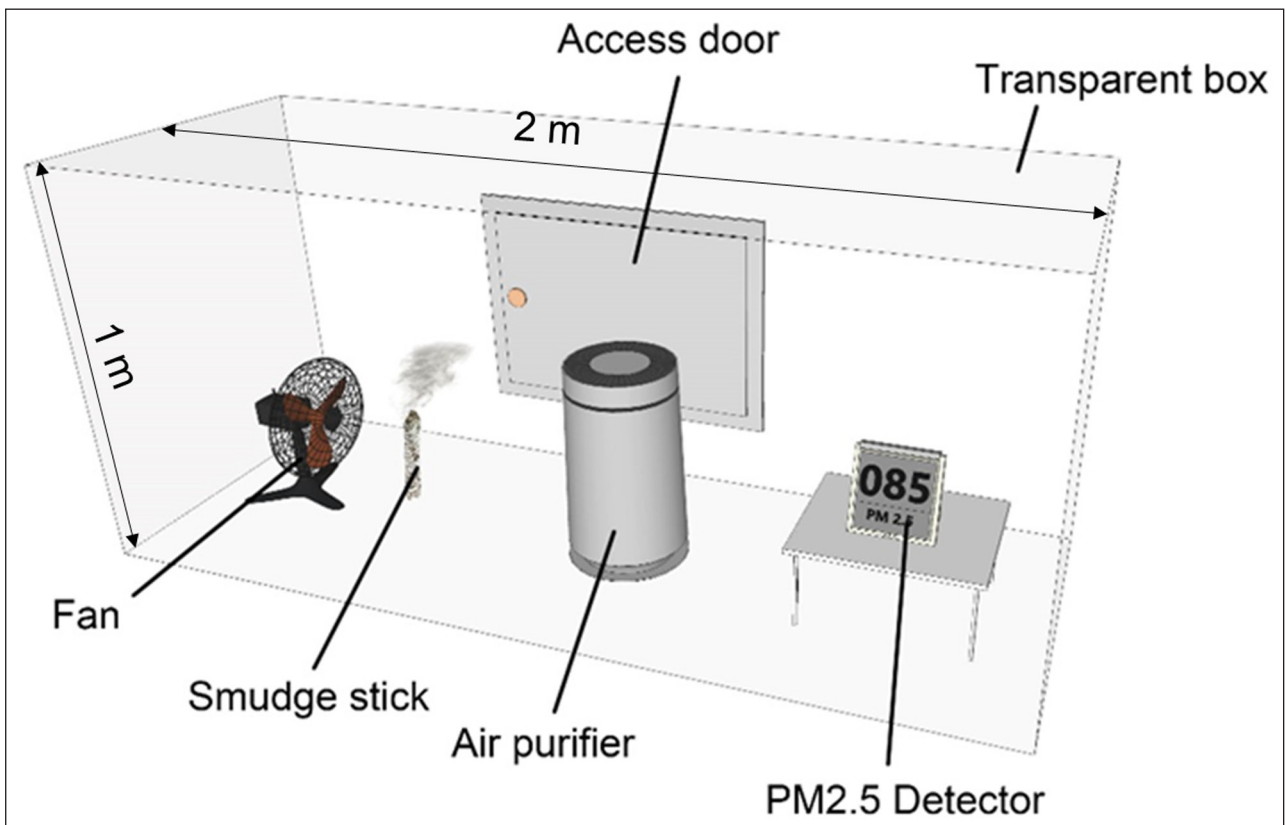


Figure 1: Schematic illustration of lab-build PM adsorption test system.

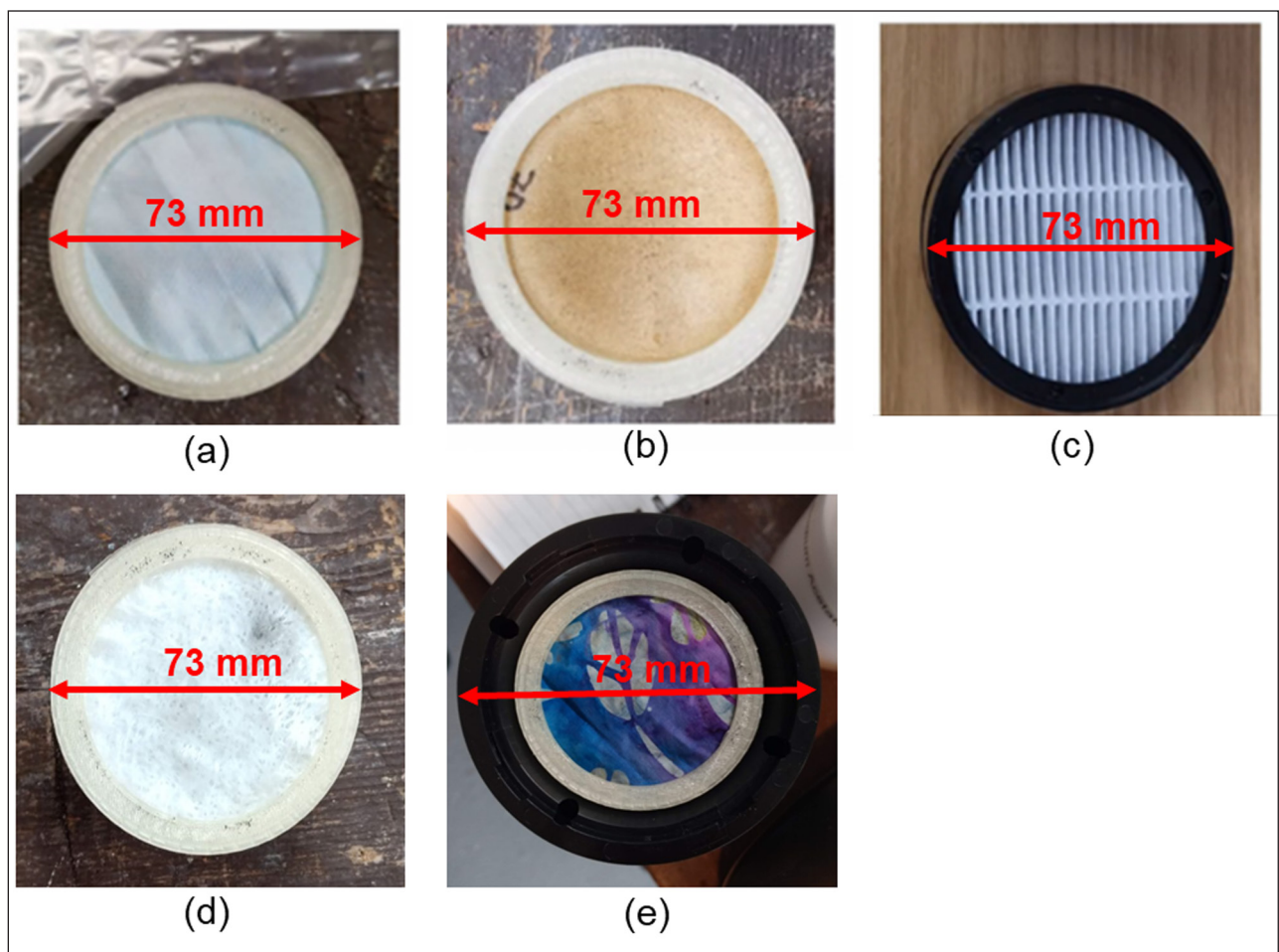


Figure 2: Images of all filter samples (a) surgical mask; (b) biomass-based aerogel; (c) HEPA; (d) silica aerogel and (e) regular cloth.

ing particles with different sizes were captured and measured by a PM detector (LKC-1000S+, TEMTOP multifunctional air quality meter). The PM 2.5 and PM 10 mass concentrations were recorded by detector. In addition, there are some limitations of equipment existing in this experiment including the limitation of the maximum PM concentrations. Both PM 2.5 and PM 10 removal efficiency of filter materials was calculated according to Yan et al. (2019) as below (Eq. 1):

$$\text{Removal efficiency} = 1 - C_2/C_1 \times 100\% \quad (\text{Eq. 1})$$

where C1 represents the PM mass concentration before the start of air purifier and C2 represents the PM mass concentration after the start of air purifier.

2.4.4. Real room filtration tests

To further evaluate the PM filtration efficiency in practical applications, real room filtration tests have been carried out in a small room as shown in **Figure 3**. During the filtration test, the door and window in this room were closed to maintain the same test condition. After each test, the window and door will be opened to ventilate for the next test. Two smudge sticks, an air purifier (2415112EU, Leitz TruSens Z-1000 Air Purifier) with different filtration materials were placed on the table at the room corner.

For this real room test, the burning smudge sticks were used as the pollutant, and a PM detector was used for particulate matter concentration detection. In this test, the entire process was recorded, which could be divided into three stages: 1) the beginning stage of smudge stick burning; 2) the stage when PM particles in the room reached the maximum; 3) the final stage after turning on the air purifier. Because of the similar properties to PMs, burning smudge sticks were used to produce a large amount of smoke, which is representative of PM particles in this test. The Air purifier was placed next to the smudge stick to purify air in the room. A PM detector was used to evaluate the gaseous pollutant removal performance of different filtration materials. The removal efficiency of filters in the real room was also calculated based on Eq. 1. Compared with the small transparent chamber filtration test, this real room experiment could represent practical air environment changes indoors.

3. Results and discussion

3.1. Microstructure characterization of different filters

The internal morphology of biomass-based aerogel is a three-dimensional porous structure as shown in **Figure 4**. With the addition of wheat straw, biomass-based aerogels showed a greenish-brown appearance before the



Figure 3: Photos of real room experiment setup.

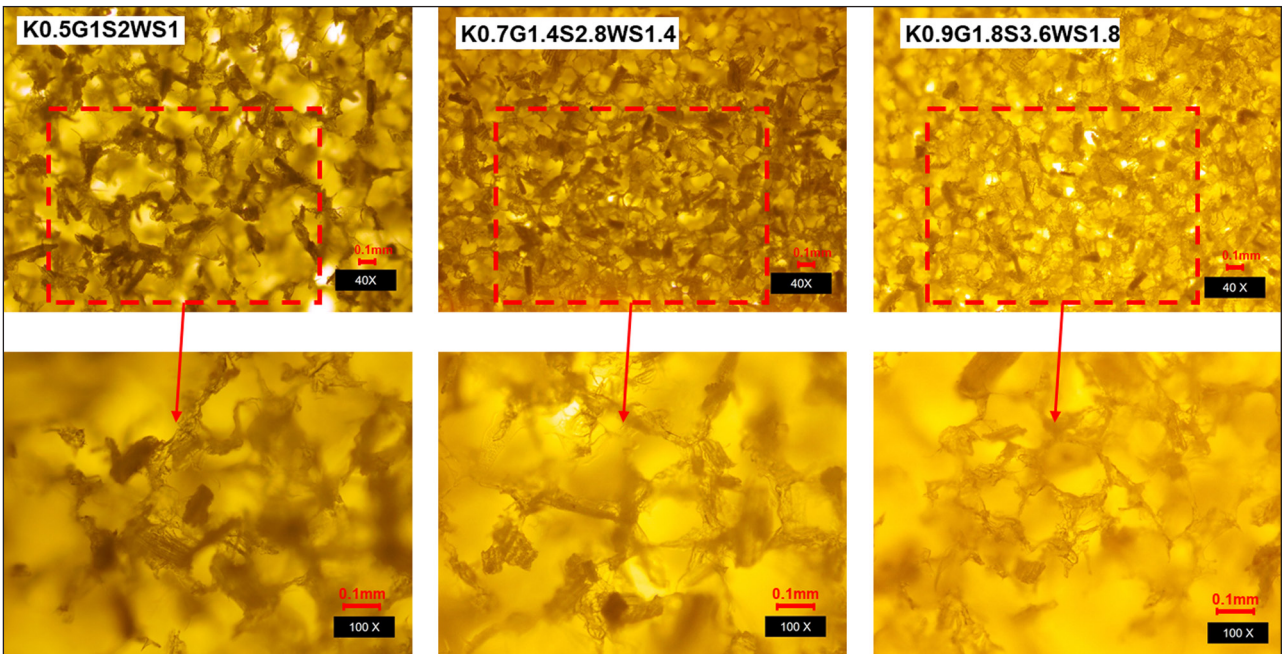


Figure 4: Micro-images of biomass-based aerogel before the filtration test.

test. It could be observed that wheat straw is randomly arranged in the pores of biomass-based aerogels. In addition, SEM was used for the observation of the internal structure details to ensure that wheat straw is evenly distributed inside the matrix thereby maximizing the surface area and the potential for PM filtration. From

Figure 5, it could be found that the pore sizes of biomass-based aerogels with three different solid concentrations are different. The pore size of biomass-based aerogels began to have a significant increase with the increase of total solid concentration. The multi-cavities structure of wheat straw could be clearly observed, which contributes

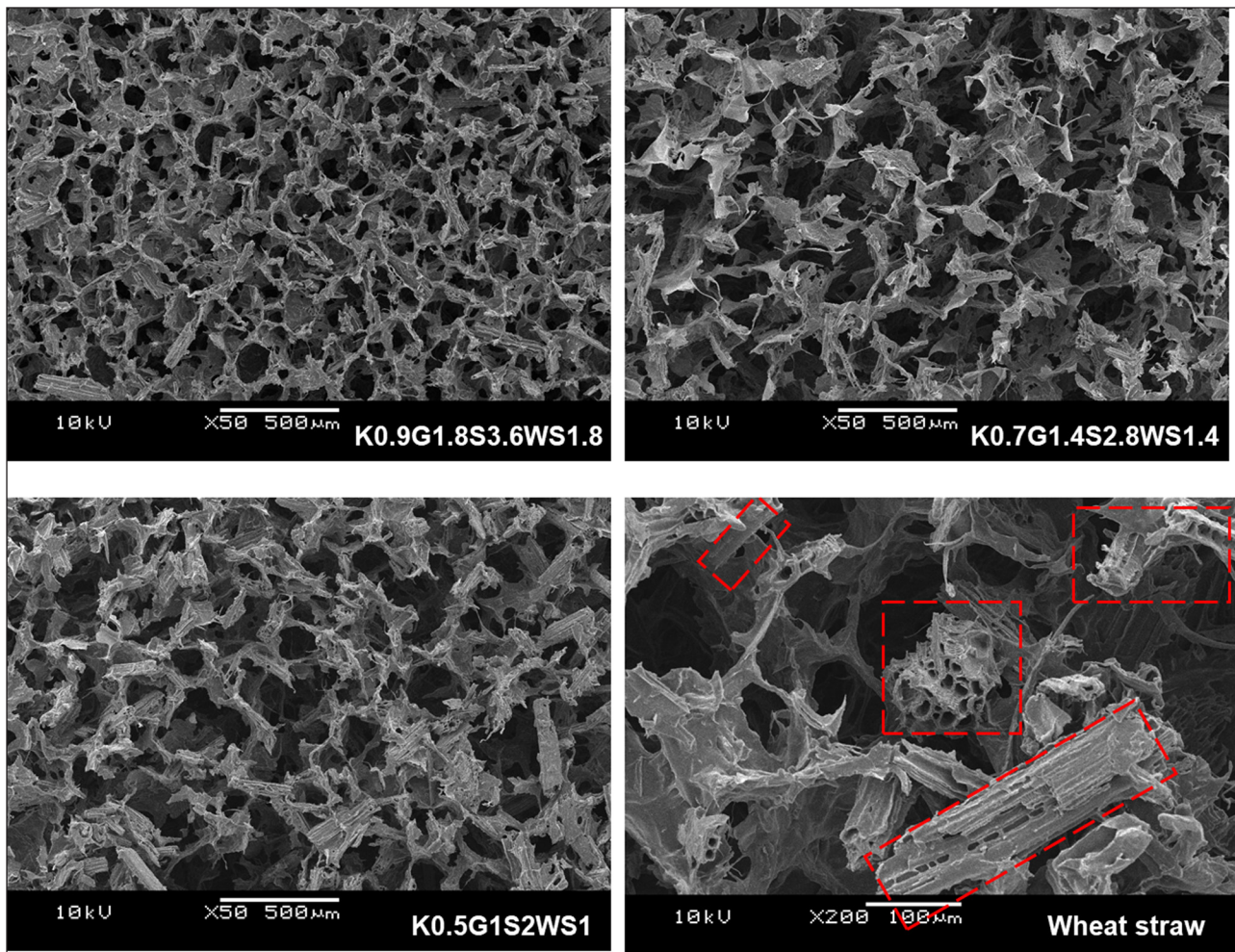


Figure 5: SEM-images of biomass-based aerogel before the filtration test.

to the increase of tiny holes in biomass-based aerogels and makes the biomass-based aerogel pore structure more complicated.

After filtration test, color of the biomass-based aerogel has been changed significantly, and it was stained red-brown by smoke. Due to the small size of particles, they cannot be fully observed. But as illustrated in **Figure 6**, the intercepted large PM particles can be observed by microscope. In **Figures 6** and **7**, the particle sizes were measured using Image-Pro Plus 6.0 and the diameters of particles range from 7.1 to 62.8 μm .

The same test has also been carried out with the melt-blown fabrics and non-woven fabrics and both are thin layers with a two-dimensional structure. As shown in **Figure 7**, the structure of the melt-blown cloth is dense, and few holes can be observed. However, there are too many open spaces in the fibres of non-woven fabric, which can allow particles to pass through. PM particles could be observed in these two fabrics, but the particles on non-woven fabrics are relatively less than melt-blown fabrics and biomass-based aerogels. The SEM images of different filters are presented in **Figure 8**. As demonstrated, the pore size of non-woven fabric and silica aerogel is larger than that of melt-blown fabric, regular cloth and biomass-based aerogel K0.9G1.8S3.6WS1.8. The multi-cavities structure of wheat straw also could be found in the biomass-based aerogels.

3.2. PM filtration performance test in the transparent chamber

As introduced in section 2.4.3, the PM filtration performance was measured by using a handmade transparent chamber with a small fan, smudge stick, air purifier and PM detector. In this study, the PM 2.5 and PM 10 filtration efficiency of different filters was calculated by comparing the particle concentration before and after the start of air purifier. Every test lasted one hour, during the first 30 minutes the smudge stick was burned completely. In the next 30 minutes, the particle concentrations were measured and the data was recorded every minute. With the work of different filters, PM particles have been removed at different rates. As shown in **Figure 9**, the filters have good filtration performance compared with regular cloth and silica aerogel. In the beginning, there are full of particles in the transparent chamber and the filtration efficiencies of all samples are zero in the first five minutes. At the fifth minute, the curve for HEPA starts to increase dramatically, converges gradually and finally reaches the highest filtration efficiency of 98.80% at the thirtieth minute. Compared with the HEPA filter, a one-minute delay can be observed for three types of biomass-based aerogels to start to remove particles. Biomass-based aerogel K0.9G1.8S3.6WS1.8 shows a similar growth rate with HEPA at the beginning, but its growth rate begins to exceed HEPA at around 15 minutes. At last, the removal

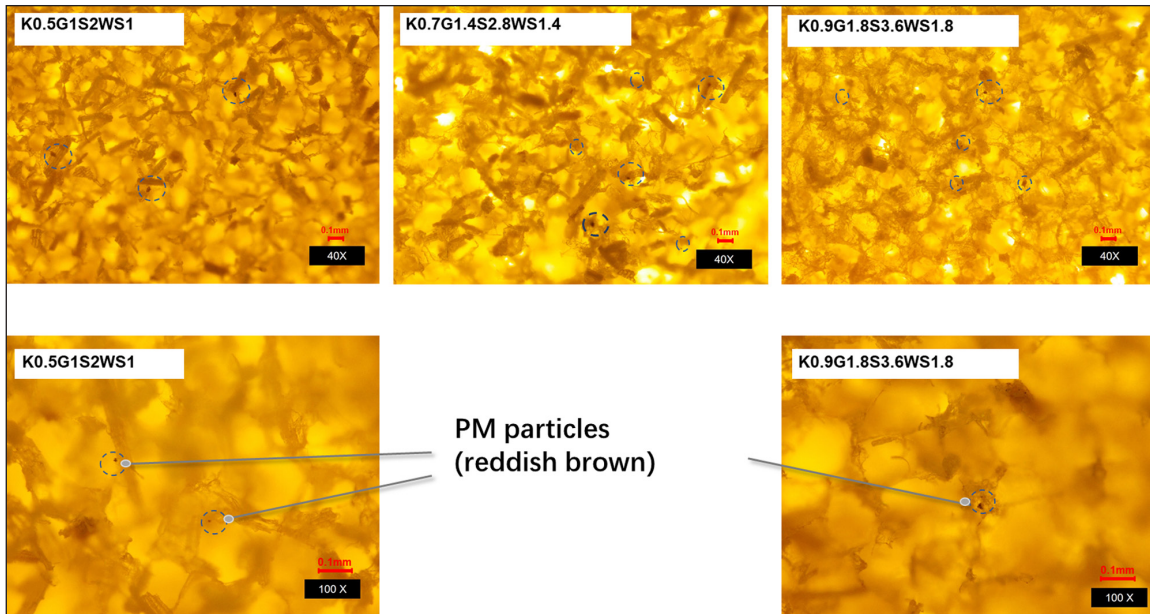


Figure 6: Micro-image of biomass-based aerogel after the filtration test (K, S, G and WS represent konjac glucomannan, potato starch, gelatin, wheat straw, respectively; the number after K, S, G and WS indicates the weight volume percent of composition in the original sol.).

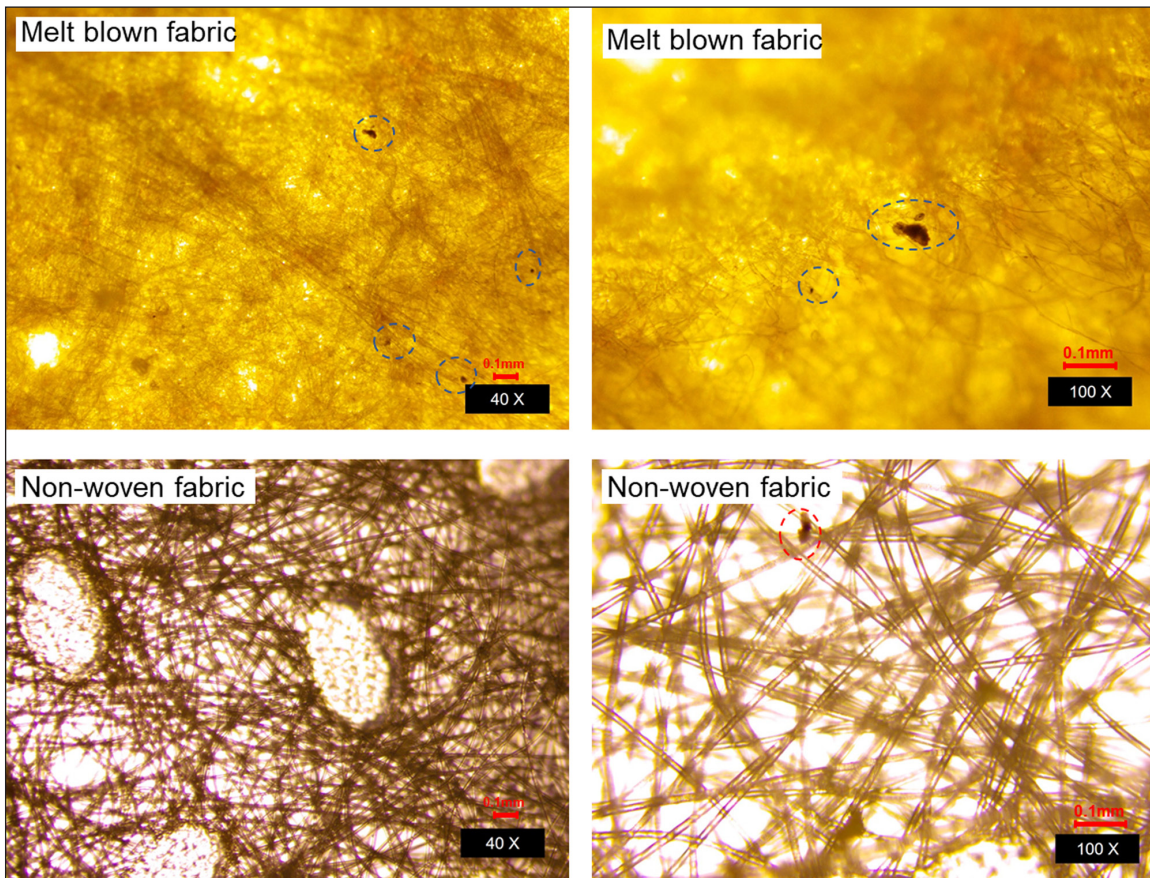


Figure 7: Micro-image of melt-blown fabric and non-woven fabric after the filtration test.

efficiency of K0.9G1.8S3.6WS1.8 reaches 99.50% at the thirtieth minute, which is the highest among all filters. On the other hand, the filtration performance of K0.5G1S2WS1 is worse than the other two biomass-based aerogels (89.79%) because it has low solid concentration,

which results in the low density and a large number of open pores in the structure of biomass-based aerogels. The particle removal efficient rates of three biomass-based aerogels are different. With a high density and relatively dense structure, the K0.9G1.8S3.6WS1.8 has the highest

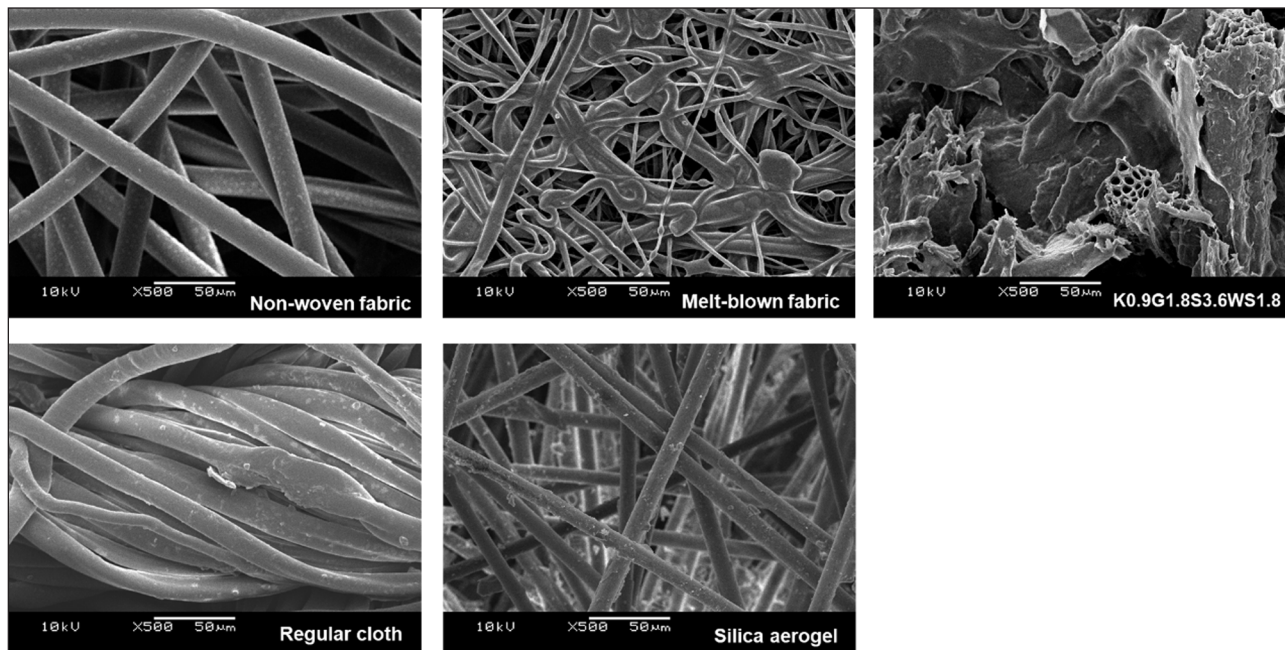


Figure 8: SEM-images of melt-blown fabric, non-woven fabric, biomass-based aerogel, regular cloth and silica aerogel after the filtration test.

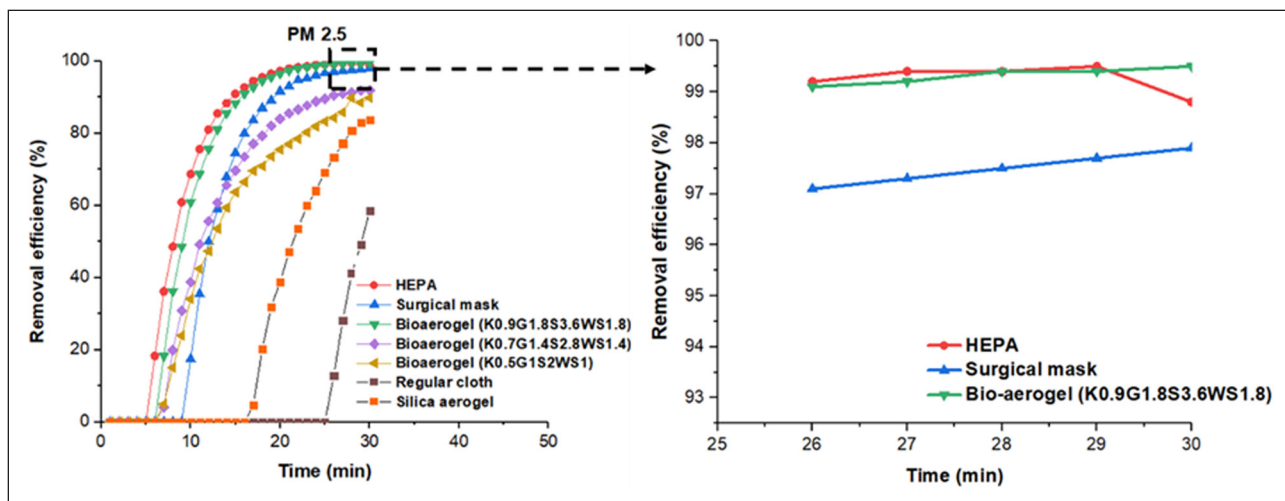


Figure 9: The PM 2.5 removal efficiency of (a) different filters from 0 min to 30 min, (b) HEPA, surgical mask and biomass-based aerogel K0.9G1.8S3.6WS1 from 26min to 30 min (K, S, G and WS represent konjac glucomannan, potato starch, gelatin, wheat straw, respectively; the number after K, S, G and WS indicates the weight volume percent of composition in the original sol.).

growth rate followed by the K0.7G1.4S2.8WS1.4. In the beginning, there is a difference in their growth rate and this difference between them becomes more obvious as the experiment continued. At the end of the test, PM 2.5 removal efficiency of K0.7G1.4S2.8WS1.4. is 89.79%. At the ninth minute, the surgical mask starts to work and has a similar growth rate of HEPA and K0.9G1.8S3.6WS1.8. At the end of the test, the removal efficiency of surgical mask reached 97.90%, which means good PM 2.5 filtration performance. To be more specific, **Figure 9(b)** was used to magnify the details and compare PM 2.5 removal efficiency of HEPA, surgical mask and biomass-based aerogel K0.9G1.8S3.6WS1 from 26 minutes to 30 minutes. It could be found that the filtration efficiency of

HEPA decreases at the 30th minute, while the filtration efficiency of biomass-based aerogel K0.9G1.8S3.6WS1.8 continuously increases and eventually higher than that of HEPA at the end. In this test, the two worst removal efficiencies were observed with silica aerogel (83.78%) and regular cloth (58.56%). To confirm the effect of particle sizes, the filtration tests of PM 10 were also studied, and the results are shown in **Figure 10**. Compared with the removal test of PM 2.5, the removal efficiency curve of PM 10 has a similar tendency, in which the filtration performance of HEPA and biomass-based aerogel K0.9G1.8S3.6WS1 (99.40%) are better than other filters with a relatively high growth rate. If removal efficiency of 97% is taken as the standard, the K0.9G1.8S3.6WS1, HEPA

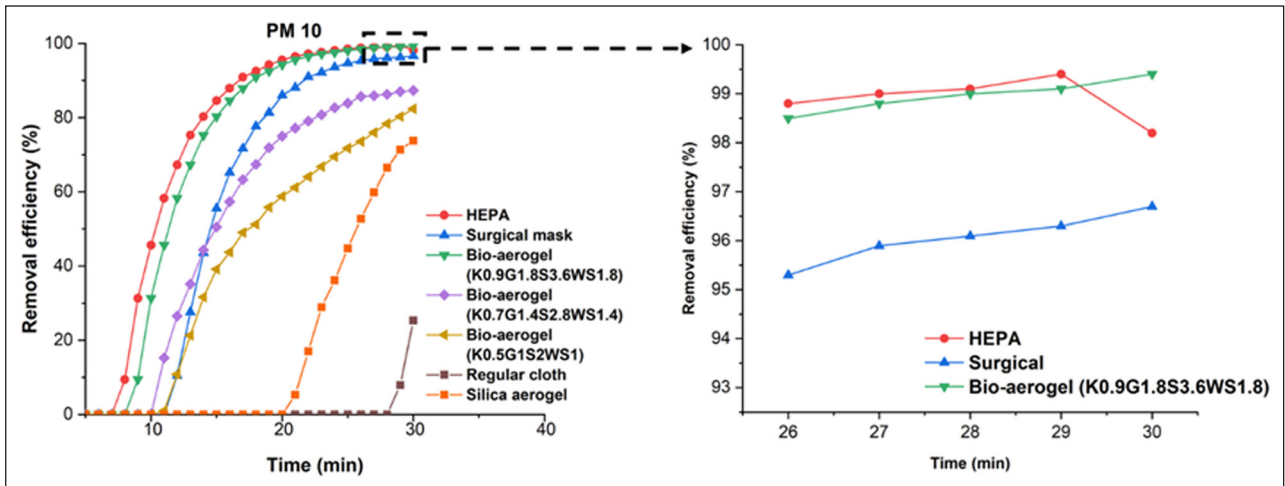


Figure 10: The PM 10 removal efficiency of (a) different filters from 0 min to 30 min, (b) HEPA, surgical mask and biomass-based aerogel K0.9G1.8S3.6WS1 from 26 min to 30 min.

can meet the requirement. The removal efficiencies reach as high as above 99% for both PM 2.5 and PM 10 for biomass-based aerogel with the formula K0.9G1.8S3.6WS1. The high promised removal efficiencies for PM 2.5 and PM 10 are attributed to the composite pore structure, the high specific surface area formed by the specific structure of wheat straw and the freeze-drying method. In the freeze-drying process, the pores were formed by the ice crystals sublimation and the pore wall was composed of solid materials. The porous structure of biomass-based aerogel provides a good foundation for filtration performance. With the addition of wheat straw, the internal structure becomes more complicated due to the special multi-cavities structure of wheat straw (as shown in Figure 5). When particles entered the biomass-based aerogels, most of them will be intercepted inside the biomass-based aerogels because of the complicated 3D structure leading to higher filtration performance. Besides, for K0.7G1.4S2.8WS1.4, K0.5G1S2WS1, silica aerogel and regular cloth, there is a little difference in the filtration efficiency between PM 2.5 and PM 10. The efficiency of removing PM 2.5 with regular cloth (58.56%) is higher than the efficiency of using it to remove PM 10 (25.33%), and this difference was significant as shown in Figure 9(a) and Figure 10(a).

3.3. Monitoring of indoor ambient air quality with different filters

The detailed PM 2.5, PM 10 concentrations were recorded, removal efficiencies were calculated following the procedure as above, and the results are shown in Figures 11 and 12. As demonstrated by the purple curve in Figure 11(a), PM 2.5 concentration by biomass-based aerogel (K0.7G1.4S2.8WS1.4 and K0.9G1.8S3.6WS1.8) increases sharply in the first 14 minutes, followed by constant high values for 30 minutes, and then drops dramatically after the forty-fifth minute under the filtration effect of biomass-based aerogel K0.7G1.4S2.8WS1.4 and K0.9G1.8S3.6WS1.8. The reason for the occurrence of constant high values from 15th min to 43rd min is the limitation of detector that the maximum PM concentra-

tion it can measure is 999. On the other hand, the PM 2.5 concentration by HEPA shows a different trend, which increases to a peak value and decreases rapidly afterward at the twenty-fifth minute. Figure 11(b) shows the PM 2.5 removal efficiency of HEPA and two biomass-based aerogels. In the real room test, the PM 2.5 removal efficiency of HEPA, biomass-based aerogel K0.9G1.8S3.6WS1.8 and K0.7G1.4S2.8WS1.4 exhibits a continuously increasing trend and final reaches 99.40%, 97.90% and 97.50%, respectively. These results are similar to filtration testing results in the transparent chamber, which shows an improvement for HEPA and biomass-based aerogel K0.7G1.4S2.8WS1.4. However, for biomass-based aerogel K0.9G1.8S3.6WS1.8, it shows a slight reduction of filtration efficiency in the real room compared with transparent chamber. To be specific, the filtration test of biomass-based aerogel K0.7G1.4S2.8WS1.4 in the real room can bring improvement of removal efficiency by 6.11%, and the biomass-based aerogel K0.9G1.8S3.6WS1.8 in the real room can bring a slight reduction of removal efficiency by 1.61%. Compared with the HEPA filter, biomass-based aerogel K0.7G1.4S2.8WS1.4 and K0.9G1.8S3.6WS1.8 have a 16-minute and 17-minute delay to start to remove particles, respectively. After the start, the removal efficiency of biomass-based aerogel K0.9G1.8S3.6WS1.8 has a similar increase rate with HEPA, while the removal efficiency increases of biomass-based aerogel K0.7G1.4S2.8WS1.4 shows a much slower trend.

Meanwhile, Figure 12 shows the PM 10 concentration and removal efficiency during the whole testing process. The HEPA is usually made of chemical fibers or glass fibers, with a diameter of about 0.5 μm to 2 μm, which is smaller than PM 10 particles. In general, the interception dominates to achieve the filtration efficiency when the particles have a larger size than the fiber diameter. It can be found in Figure 12(a) that PM 10 concentration in the real room was decreased rapidly when started to use HEPA as the filter. Meanwhile, the filtration rate of the biomass-based aerogel K0.9G1.8S3.6WS1.8 and K0.7G1.4S2.8WS1.4 is slower than HEPA. This could be explained that the biomass-based aerogel is a thin disc

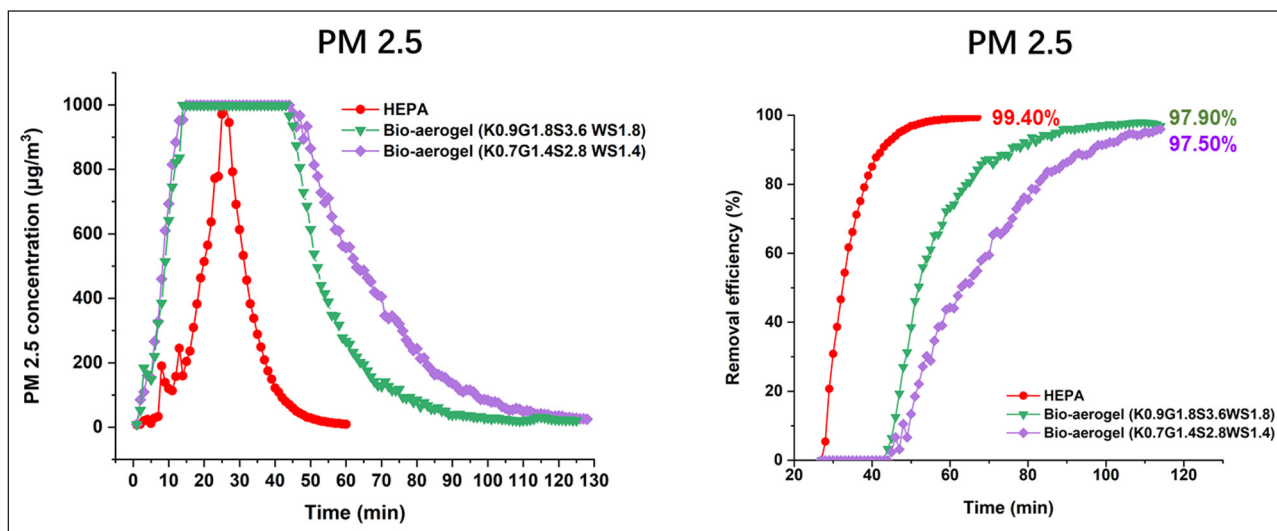


Figure 11: Measured (a) PM 2.5 concentration in the real room; and (b) PM 2.5 removal efficiency with HEPA, K0.9G1.8S3.6WS1.8 and K0.7G1.4S2.8WS1.4.

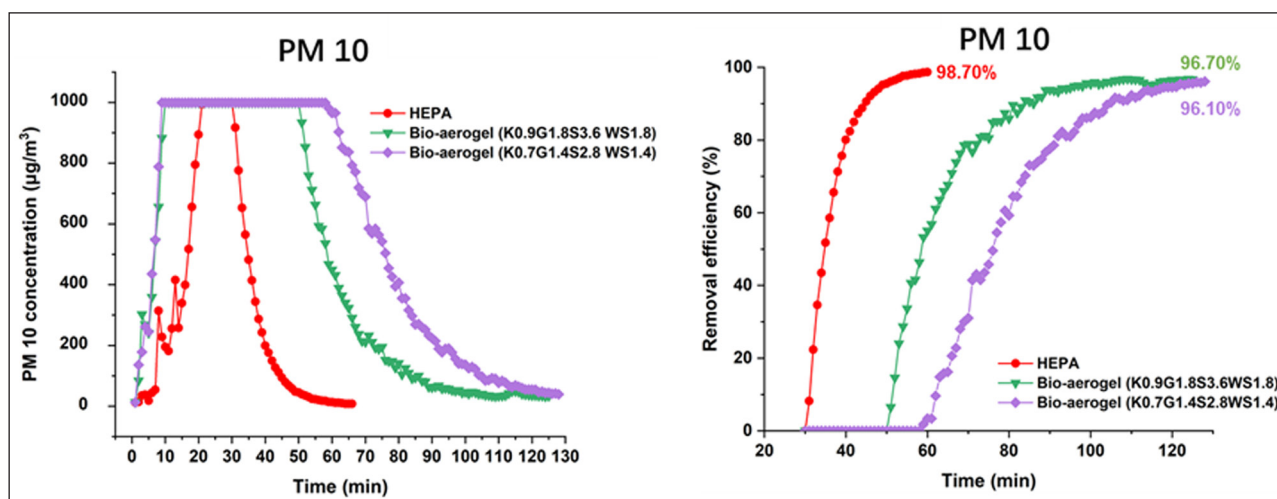


Figure 12: Measured (a) PM 10 concentration in the real room; and (b) PM 10 removal efficiency with HEPA, K0.9G1.8S3.6WS1.8 and K0.7G1.4S2.8WS1.4.

with a thickness of about 3 mm, which is much thinner than that of HEPA. Besides, the pleated HEPA structure contributes to the maximum efficiency function. When using the biomass-based aerogel, the filter core sample has a smaller volume and a simple structure. The PM 10 removal efficiency of HEPA and biomass-based aerogel K0.7G1.4S2.8WS1.4 were 98.70% and 96.10%, respectively. Compared with the same test carried out in the transparent chamber, the filtration efficiency results of biomass-based aerogel K0.7G1.4S2.8WS1.4 in the real room can bring improvement of removal efficiency by 10.09%, and K0.9G1.8S3.6WS1.8 in the real room can bring a slight reduction of removal efficiency by 2.72%. The PM 2.5 and PM 10 removal efficiency results indicate that biomass-based aerogels K0.9G1.8S3.6WS1.8 and K0.7G1.4S2.8WS1.4 show good particle filtration performance. Moreover, 3 mm thickness biomass-based aerogels K0.9G1.8S3.6WS1.8 shows similar PM removal performance to commercial product HEPA (40 mm thickness).

4. Conclusion

Biomass-based aerogels were successfully fabricated by the freeze-drying method with relatively low energy consumption. The complex 3D porous structure of biomass-based aerogels provides the condition and leads to good filtration performance. The addition of wheat straw improves surface area of biomass-based aerogel and affects the aerogel pore structure due to its special multi-cavity structure. The filtration performance comparison between biomass-based aerogels and some current commercial filters indicates the great potential of biomass-based aerogels as filtration materials for removing PM 2.5 and PM 10 in different fields. PM 2.5 and PM 10 removal efficiencies of biomass-based aerogel K0.9G1.8S3.6WS1.8 in a small transparent chamber have been determined to be 99.50% and 99.40%, respectively. HEPA shows a similar effect having removal efficiencies of 98.80 for PM 2.5 and 98.20% for PM 10. However, in terms of size, the HEPA filter is much thicker than biomass-based aerogels, and its maximum efficiency func-

tion is contributed by additional manufactured pleated HEPA structure. Using biomass-based aerogel, the filter core sample has a smaller volume and simpler structure. When compared with the surgical mask, silica aerogel and regular cloth, a thin disc of biomass-based aerogel K0.9G1.8S3.6WS1.8 as the filter is much more efficient in removing PM. The same tests have also been carried out in a real room to verify the authenticity and validity of filtration results in the transparent chamber. In the real room, both the biomass-based aerogel K0.7G1.4S2.8WS1.4 and HEPA were able to approach more favorable filtration performance than the testing results in the transparent chamber. Although biomass-based aerogel K0.9G1.8S3.6WS1.8 shows a slight reduction of filtration efficiency in the real room, PM 2.5 removal efficiency is still higher than 97%. This new environmentally friendly and efficient biomass-based aerogel has a great potential to be used as an air pollutant filter with excellent filtration properties.

Acknowledgements

This research is financially supported by the Innovate UK funding (Project Grant ID: 78047). The authors would like to thank the continued technical support from Nicola Weston and Elisabeth Steer at the Nanoscale and Microscale Research Centre (nmRC), University of Nottingham.

Competing Interests

Saffa Riffat is the Editor in Chief of the journal and was removed from all editorial processing for this paper.

Author Contributions

Yixin Wang: Methodology, Data curation, Formal analysis, Investigation, Writing- original draft preparation. Emmanuel Tapia Brito: Methodology, Data curation, Review and editing. James Riffat: Methodology and Data curation. Ziwei Chen: Review and editing. Fatang Jiang: Resources, Review and editing. Saffa Riffat: Conceptualization, Resources, Review and editing, Project administration; Supervision. All authors have read and agreed to the published version of the manuscript.

References

- Behera, SS and Ray, RC.** 2016. Konjac glucomannan, a promising polysaccharide of *Amorphophallus konjac* K. Koch in health care. *International Journal of Biological Macromolecules*, 92: 942–956.
- Buggy, AK, McManus, JJ, Brodkorb, A, Hogan, SA and Fenelon, MA.** 2018. Pilot-scale formation of whey protein aggregates determine the stability of heat-treated whey protein solutions—Effect of pH and protein concentration. *Journal of Dairy Science*, 101(12): 10819–10830. DOI: <https://doi.org/10.3168/jds.2017-14177>
- Ge, H, Wu, Y, Woshnak, LL and Mitmesser, SH.** 2021. Effects of hydrocolloids, acids and nutrients on gelatin network in gummies. *Food Hydrocolloids*, 113: 106549.
- Groult, S, Buwalda, S and Budtova, T.** 2021. Pectin hydrogels, aerogels, cryogels and xerogels: influence of drying on structural and release properties. *European Polymer Journal*, 110386.
- Guilherme, EdO, de Souza, CW, Bernardo, MP, Zenke, M, Mattoso, LH and Moreira, FK.** 2021. Antimicrobially active gelatin/[Mg-Al-CO₃]-LDH composite films based on clove essential oil for skin wound healing. *Materials Today Communications*, 27: 102169.
- Jia, C, Liu, Y, Li, L, Song, J, Wang, H, Liu, Z, Wu, H, et al.** 2020. A Foldable All-Ceramic Air Filter Paper with High Efficiency and High-Temperature Resistance. *Nano Letters*, 20(7): 4993–5000. DOI: <https://doi.org/10.1021/acs.nanolett.0c01107>
- Jiang, F.** 2013. Plant polysaccharide cigarette filter tip and preparation method there of [(Pattern NO.; 1; 102423132). CN].
- Jiang, F.** 2020a. Plant polysaccharide aerogel sound absorption and noise reduction and preparation method there of [(Pattern NO.; 108285556). CN].
- Jiang, F.** 2020b. Plant polysaccharide thermal insulation aerogels material and preparation method thereof [(Pattern NO.; 108285549). CN].
- Leung, WWF and Sun, Q.** 2020. Electrostatic charged nanofiber filter for filtering airborne novel coronavirus (COVID-19) and nano-aerosols. *Separation and purification technology*, 250: 116886.
- Li, M and Fu, S.** 2021. Photochromic holo-cellulose wood-based aerogel grafted azobenzene derivative by SI-ATRP. *Carbohydrate Polymers*, 259: 117736.
- Liu, H, Liu, L, Yu, J, Yin, X and Ding, B.** 2020. High-efficiency and super-breathable air filters based on biomimetic ultrathin nanofiber networks. *Composites Communications*, 22: 100493.
- Lv, S, Zhao, X, Shi, L, Zhang, G, Wang, S, Kang, W and Zhuang, X.** 2018. Preparation and properties of sc-PLA/PMMA transparent nanofiber air filter. *Polymers*, 10(9): 996. DOI: <https://doi.org/10.3390/polym10090996>
- Mandal, S and Srimani, B.** 1987. Jute fiber as a filter medium in microbial air filters. *Annals of the New York Academy of Sciences*, 506: 682–688.
- Meng, X, Zhang, Y, Yang, K-Q, Yang, Y-K and Zhou, X-L.** 2016. Potential harmful effects of PM_{2.5} on occurrence and progression of acute coronary syndrome: epidemiology, mechanisms, and prevention measures. *International journal of environmental research and public health*, 13(8): 748. DOI: <https://doi.org/10.3390/ijerph13080748>
- Qiao, S, Kang, S, Zhu, J, Wang, Y, Yu, J and Hu, Z.** 2021. Facile strategy to prepare polyimide Nanofiber assembled aerogel for effective airborne particles filtration. *Journal of Hazardous Materials*, 125739.
- Rajak, A, Hapidin, DA, Iskandar, F, Munir, MM and Khairurrijal, K.** 2020. Electrospun nanofiber from various source of expanded polystyrene (EPS) waste and their characterization as potential air filter media. *Waste Management*, 103: 76–86.
- Selmer, I, Kleemann, C, Kulozik, U, Heinrich, S and Smirnova, I.** 2015. Development of egg white protein aerogels as new matrix material for

microencapsulation in food. *The Journal of Supercritical Fluids*, 106: 42–49.

- Ubeyitogullari, A and Ciftci, ON.** 2016. Formation of nanoporous aerogels from wheat starch. *Carbohydrate Polymers*, 147: 125–132.
- Wang, L, Sánchez-Soto, M and Abt, T.** 2016. Properties of bio-based gum Arabic/clay aerogels. *Industrial Crops and Products*, 91: 15–21.
- Wang, W, Fang, Y, Ni, X, Wu, K, Wang, Y, Jiang, F and Riffat, SB.** 2019. Fabrication and characterization of a novel konjac glucomannan-based air filtration aerogels strengthened by wheat straw and okara. *Carbohydrate Polymers*, 224: 115129.
- Wang, Y, Chen, X, Kuang, Y, Xiao, M, Su, Y and Jiang, F.** 2019. Microstructure and filtration performance of konjac glucomannan-based aerogels strengthened by wheat straw. *International Journal of Low-Carbon Technologies*, 14(3): 335–343. DOI: <https://doi.org/10.1093/ijlct/ctx021>
- Wang, Y, Su, Y, Wang, W, Fang, Y, Riffat, SB and Jiang, F.** 2019. The advances of polysaccharide-based aerogels: Preparation and potential application. *Carbohydrate Polymers*, 226: 115242.
- Wang, Y, Wu, K, Xiao, M, Riffat, SB, Su, Y and Jiang, F.** 2018. Thermal conductivity, structure and mechanical properties of konjac glucomannan/starch based aerogel strengthened by wheat straw. *Carbohydrate Polymers*, 197: 284–291.
- Wu, K, Fang, Y, Wu, H, Wan, Y, Qian, H, Jiang, F and Chen, S.** 2021. Improving konjac glucomannan-based aerogels filtration properties by combining aerogel pieces in series with different pore size distributions. *International Journal of Biological Macromolecules*, 166: 1499–1507.
- Xie, Y, Guo, F, Mao, J, Huang, J, Chen, Z, Jiang, Y and Lai, Y.** 2021. Freestanding MoS₂@ carbonized cellulose aerogel derived from waste cotton for sustainable and highly efficient particulate matter capturing. *Separation and purification technology*, 254: 117571.
- Yan, S, Zhang, G, Li, F, Zhang, L, Wang, S, Zhao, H, Li, H, et al.** 2019. Large-area superelastic graphene aerogels based on a room-temperature reduction self-assembly strategy for sensing and particulate matter (PM 2.5 and PM 10) capture. *Nanoscale*, 11(21): 10372–10380. DOI: <https://doi.org/10.1039/C9NR02071C>
- Yin, Z, Sun, X, Bao, M and Li, Y.** 2020. Construction of a hydrophobic magnetic aerogel based on chitosan for oil/water separation applications. *International Journal of Biological Macromolecules*, 165: 1869–1880.
- Zare Shahneh, A.** 2020. Improving aircraft cabin air quality by reducing Tri-Cresylic Phosphate.
- Zhang, S, Sun, J, Hu, D, Xiao, C, Zhuo, Q, Wang, J, Dai, L, et al.** 2018. Large-sized graphene oxide/modified tourmaline nanoparticle aerogel with stable honeycomb-like structure for high-efficiency PM 2.5 capture. *Journal of Materials Chemistry A*, 6(33): 16139–16148. DOI: <https://doi.org/10.1039/C8TA05506H>
- Zhao, K, Huang, J, Mao, J, Bao, Z, Chen, Z and Lai, Y.** 2020. Charged graphene aerogel filter enabled superior particulate matter removal efficiency in harsh environment. *Chemical Engineering Journal*, 395: 125086.
- Zhuang, J, Dai, J, Ghaffar, SH, Yu, Y, Tian, Q and Fan, M.** 2020. Development of highly efficient, renewable and durable alginate composite aerogels for oil/water separation. *Surface and Coatings Technology*, 388: 125551.
- Zoran, MA, Savastru, RS, Savastru, DM and Tautan, MN.** 2020. Assessing the relationship between surface levels of PM_{2.5} and PM₁₀ particulate matter impact on COVID-19 in Milan, Italy. *Science of the total environment*, 738: 139825.

How to cite this article: Wang, Y, Tapia-Brito, E, Riffat, J, Chen, Z, Jiang, F and Riffat, S. 2021. Investigation on the Efficient Removal of Particulate Matter (PM) with Biomass-Based Aerogel. *Future Cities and Environment*, 7(1): 12, 1–12 DOI: <https://doi.org/10.5334/fce.131>

Submitted: 08 June 2021

Accepted: 08 August 2021

Published: 24 August 2021

Copyright: © 2021 The Author(s). This is an open-access article distributed under the terms of the Creative Commons Attribution 4.0 International License (CC-BY 4.0), which permits unrestricted use, distribution, and reproduction in any medium, provided the original author and source are credited. See <http://creativecommons.org/licenses/by/4.0/>.

]u[

Future Cities and Environment, is a peer-reviewed open access journal published by Ubiquity Press.

OPEN ACCESS 